Atmospheric Vorticity Production in Electrified Clouds

J. DOYNE SARTOR[1] AND JOHN H. HELSDON, JR.[2]

National Center for Atmospheric Research,[3] Boulder, CO 80307

(Manuscript received 13 June 1980, in final form 29 July 1981)

ABSTRACT

The rate that vertical vorticity is created or retarded in electrified clouds is calculated from the cross product of the charge gradient and the electrical field and compared with the magnitude of the vertical vorticity produced dynamically. Calculations are made for clouds on the thunderstorm, mesoscale and synoptic scales for midlatitude and tropical conditions. The results show that in moderately electrified clouds with particle charges an order of magnitude less than the observed maxima, the production of vorticity due to electrostatic forces approaches or slightly exceeds the dynamic production in thunderstorm anvil clouds and on the mesocale in the tropics. Highly electrified clouds with maximum particle charges can produce vorticity at comparable rates to its dynamic production on all scales except the synoptic scale in midlatitudes.

To the extent that cloud charging conditions due to the global electric field and mid-tropospheric conductivity conditions are perturbed by solar events or solar-included electromagnetic disturbances, some solar influence on the electrical conditions could be expected in the mid-troposphere where clouds of the suitable type and extent form as a consequence of the normal meteorological processes. Where the electrical conditions exceed the threshold required for the production of vorticity dynamically, organized circulations produced electrophysically are possible in a solar-disturbed large-scale electrical environment.

1. Introduction

Very recently there has been a renewed interest in the response of the weather and atmospheric circulation to solar events that cause perturbations in the global electrical properties of the troposphere (Herman and Goldberg, 1978; Markson, 1978; National Science Foundation, 1978). This has been partly due to statistical studies correlating solar electromagnetic changes and the vorticity area index (VAI) (Roberts and Olson, 1973); and partly to physical and numerical models of the electrical processes in the global electrical environment (Hays and Roble, 1979) and the progressive improvement over the past 10–12 years in the modeling of the role of the global electrical field in thunderstorm electrification (Sartor, 1967a; Mason, 1972; Paluch and Sartor, 1973; Scott and Levin, 1975; Chiu, 1978).

Markson's hypothesis (Markson, 1978) rests on an argument that solar modulations of atmospheric conductivity change the earth's electric field intensity, affecting the intensity of thunderstorm electrification over extensive regions of the earth which, in turn, acts to produce more precipitation more rapidly, indirectly affecting the subsequent circulation patterns. Numerous other cloud physical processes also were mentioned (e.g., changes in albedo, seeding of lower downwind clouds, etc.). The circulation changes are evidenced in statistical studies relating vorticity to solar modulations in the electromagnetic and magneto-hydrodynamic perturbations in the solar particle output, (Roberts and Olson, 1973). In this paper the production of vorticity as a consequence of charged particle motions in the electric fields in clouds is computed and found to be significant in some meteorological situations.

The first step in the argument, that solar activity modulates the global electric circuit, receives support from observations at high-altitude mountain stations in Bavaria (Reiter, 1969, 1971) and on Mauna Loa, Hawaii (Cobb, 1967). Observations on Niwot Ridge, Colorado, bear out a similar modulation but suggest a longer period of meteorological interaction (Sartor, 1980). Radio transmissions via sporadic *E* in the southeastern United States were observed in the vicinity of Key West, Florida, during the summer of 1964 (Sartor, 1967b) that apparently were related to heavy thunderstorm precipitation between the receiving station at Key

[1] Deceased.

[2] The material for this paper was written by Doyne Sartor and was found by Tzvi Gal-Chen after Sartor's death in 1979. Gal-Chen sent the material in to the *Journal of the Atmospheric Sciences* for review. The required revisions were extensive and consequently John Helsdon, who did the major revisions, is listed as a coauthor.

[3] The National Center for Atmospheric Research is sponsored by the National Science Foundation.

0022-4928/81/122763-09$06.25

West and the transmitting stations located in the continental United States. Numerous observational studies linking sporadic E occurrences to thunderstorm activity have been reported over the past 45 years. Examples of these observations are contained in references (Appleton and Naismith, 1933; Isted, 1954; Reiter, 1976).

Herman and Goldberg (1978) proposed a similar hypothesis to that of Markson (1978), which couples solar activity with the initiation of nontropical thunderstorms. They suggest that the physical link may be provided by the alteration of the electric parameters of the free atmosphere, which are a consequence of cosmic ray activity and high-energy solar protons associated with active solar events. Because of high-latitude solar proton cutoff their attention is confined to the more northern regions of the globe. For meteorological reasons, the proposed thunderstorm interaction could be stronger in tropical regions as we will see later.

A great deal of attention has been given to the problem of the electrification of thunderstorms but very little work concerning the charging processes in high-level layered and extensive cloud systems has been done. Considerable controversy has developed over the electrification of thunderstorms because usually one mechanism is considered to the exclusion of others, or at least, not calculated interactively with other processes. When several processes are considered together in a more general way (see Sartor, 1970; Chiu, 1978; Kuettner *et al.*, 1978), the situation does not become less complicated, but it does become more tractable and permits the electrification of clouds to be placed quantitatively into the Hays-Roble (1979) model of global atmospheric electrical structure.

Many of the theoretical and computational techniques used in thunderstorm models can be transferred for use in the larger-scale cloud systems. Kuettner *et al.* (1978, hereafter referred to as KLS) have developed a two-dimensional model and Chiu (1978) an axisymmetric cloud model that can be applied to extensive layer clouds and the huge anvil-like cumulonimbus clouds that often dominate much of the tropical sky. These models start by introducing a cloud and its circulation into the electrical environment as it exists on the worldwide average. The KLS model shows that the excessive charge (usually positive) is taken away in the extensive anvil and middle layer clouds produced by thunderstorms. This electrical environment is directly modified by solar emission events (Cobb, 1967; Reiter, 1971) and the effect on the global scale could be calculated employing the Hays-Robel model. Chiu (1978) computes the atmospheric ion production and its effect on the conductivity of the air, ion attachment to cloud particles, the electric field, and inductive charging of colliding and separating cloud and precipitation particles which are allowed to grow by condensation and coalescence as the cloud matures. The KLS model uses a steady-state cloud air circulation and computes the microphysical growth of cloud particles by accretion and their electrification by induction, by the most efficient freezing electrification mechanism and by their combined effect. Both KLS and Chiu conclude that, although other mechanisms may proceed more rapidly in the early stages, the induction mechanism eventually takes over and is necessary for the production of highly electrified clouds and thunderstorms. Both models show that, with a sufficiently strong initial electrical environment, clouds could become highly electrified without support from other mechanisms and that induction charging and charge transfer between colliding, separating, and combining particles must be accounted for in any cloud electrification model to get a physically reasonable result. Insofar as solar events may affect the initial electrical state in which thunderstorms form and therefore may affect the ultimate electrification produced, it remains to be investigated whether such electrification can influence the vorticity production associated with such storms, since it was studies of vorticity which helped renew interest in a possible sun–weather connection.

2. Calculations

The main purpose of this study is to test the proposition that the electrophysical forces can attain, on any scale in the atmosphere, similar orders of magnitude as the dynamic processes. If regions in the atmosphere exist where the competition is of similar magnitude, further research would be indicated. Therefore, calculations are made in a search for the maximum effect.

The equation of atmospheric motion with electrophysical forces added can be written

$$\frac{\partial \mathbf{V}}{\partial t} = \frac{\sum \mathbf{F}_D}{\rho_a} - (\mathbf{V}\cdot\nabla)\mathbf{V} - 2\boldsymbol{\Omega} \times \mathbf{V} + \frac{\rho_e \mathbf{E}}{\rho_a}, \quad (1)$$

where $\mathbf{V}$ is velocity, $2\boldsymbol{\Omega} \times \mathbf{V}$ the Coriolis acceleration, $\mathbf{F}_D$ the hydrodynamical forces per unit volume, ρ_a the density of air and $\mathbf{E}$ the electric field created by ρ_e, the charge density.

Taking the curl of both sides of Eq. (1),

$$\nabla \times \frac{\partial \mathbf{V}}{\partial t} = \nabla \times \left[\frac{\sum \mathbf{F}_D}{\rho_a} - (\mathbf{V}\cdot\nabla)\mathbf{V} - 2\boldsymbol{\Omega} \times \mathbf{V}\right] + \nabla \times \frac{\rho_e \mathbf{E}}{\rho_a}, \quad (2)$$

one obtains a vorticity equation in which it is customary in meteorology to consider only the vertical component produced directly by horizontal motions.

The first three terms on the right (within the brackets) contain all the usual meteorologically important parameters and are treated extensively in the meteorological literature (Holton, 1972). Since these terms and calculations of their magnitude are readily available in the meteorological literature, the first author evaluated only the last term on the right containing the electrophysical factors, and compared this with previous calculations of vorticity produced by hydrodynamical factors. The vorticity produced by the last term on the right is

$$\nabla = \left(\frac{\rho_e \mathbf{E}}{\rho_a}\right) = \nabla\left(\frac{\rho_e}{\rho_a}\right) \times \mathbf{E} + \frac{\rho_e}{\rho_a}(\nabla \times \mathbf{E}). \quad (3)$$

The second term on the right of this equation vanishes since $\mathbf{E}$ is the gradient of the potential. Expanding the first term,

$$\nabla\left(\frac{\rho_e}{\rho_a}\right) \times \mathbf{E} = \frac{\nabla\rho_e}{\rho_a} \times \mathbf{E} - \frac{\rho_e \nabla\rho_a}{\rho_a^2} \times \mathbf{E} \quad (3a)$$

In agreement with meteorological practice only the horizontal components of motion are considered and the vorticity calculated only in the vertical direction where $\hat{k}$ is the unit vector. The gradient of ρ_a in the horizontal direction is small compared to ρ_a itself. Only the first term on the right is kept, giving

$$\frac{\partial \eta_{e\uparrow}}{\partial t} = \left(\frac{\nabla\rho_e}{\rho_a} \times \mathbf{E}\right)\cdot\hat{k} \quad (3b)$$

for the rate of change of the vertical component of the vorticity $\partial\eta_{e\uparrow}/\partial t$ in a unit volume of air due to electrophysical forces. The magnitude of this term will be compared with the dynamic production of vertical vorticity in the atmosphere. The horizontal components of vorticity are likely to be of equal or greater magnitude, but do not offer the same opportunity for comparison as the vertical component because of its importance to meteorological processes.

Simple cloud geometries with maximum average charges and their derived electrical fields are explored for the rate of vertical vorticity production in them. An ellipsoidal charge density field that decreases in confocal shells from the foci to the outer surface can be expressed simply as

$$\rho_e = \rho_{\max}\left[1 - \left(\frac{x^2}{x_0^2} + \frac{y^2}{y_0^2} + \frac{z^2}{z_0^2}\right)\right],$$

for

$$\left(\frac{x^2}{x_0^2} + \frac{y^2}{y_0^2} + \frac{z^2}{z_0^2}\right) \leq 1$$

and

$$\rho_e = 0, \quad \text{for} \quad \left(\frac{x^2}{x_0^2} + \frac{y^2}{y_0^2} + \frac{z^2}{z_0^2}\right) > 1, \quad (4)$$

where $\rho_{\max}$ is the maximum charge density in the center of the domain represented by the ellipsoid, obtained from the summation of the products of the charges per particle Q_D and the number of particles of diameter D per unit volume, N_D

$$\rho_{\max} = \sum_{D=1}^{N} Q_D N_D.$$

The horizontal components are x and y and the vertical is z. The constants x_0, y_0 and z_0 are the semi-axes of the ellipsoid. A number of these ellipsoidal charge distributions may be superimposed and centered at different locations, permitting a generally useful formulation for atmospheric charge volumes. An extremely oblate spheroidal cloud fed continuously over a fixed height interval by charged particles from a thunderstorm at its center will contain charged cloud particles with number densities that decreases as the square of the distance from the center. By enlarging or decreasing the overall volume occupied by the charge, the charge density gradient can be adjusted, adding flexibility to this formulation.

An ellipsoidal charge density field in the plane $z = 0$ is illustrated in Fig. 1, where the unit of distance is $x_0 = 1.0$, and the other semi-axes of the ellipsoid, y_0 and z_0 are 0.5 and 0.5, respectively.

Gauss' law in differential form is

$$\nabla\cdot\mathbf{E} = \frac{\rho_e}{\epsilon_0}. \quad (5)$$

Substituting the ellipsoidal charge distribution ρ_e from Eq. (4) into Eq. (5), we have for $R^2 \leq 1$

$$\nabla\cdot\mathbf{E} = [1 - R^2]\cdot\left(\frac{\rho_{\max}}{\epsilon_0}\right) \quad (6)$$

and for $R^2 > 1$, $\nabla\cdot\mathbf{E} = 0$, where $R^2 = (x/x_0)^2 + (y/y_0)^2 + (z/z_0)^2$. By inspection, an electric field that satisfies this equation inside the ellipsoid ($R^2 \leq 1$) is

$$\mathbf{E} = \frac{\rho_{\max}}{\epsilon_0}\left\{\left[\frac{1}{3} - \frac{R^2}{5}\right][(x\hat{i} + y\hat{j} + z\hat{k})] + c_x\hat{i} + c_y\hat{j} + c_z\hat{k}\right\}, \quad (7)$$

where $\hat{i}$, $\hat{j}$, $\hat{k}$ are the unit vectors in a right-handed Cartesian coordinate system and c_x, c_y, and c_z are constants. Since there are no charges outside the ellipsoid and assuming there are no conductor or dielectric boundaries nearby to distort or superimpose fields on the inside, $c_x = c_y = c_z = 0$.

The gradient of the charge distribution inside the ellipsoid is obtained by applying the gradient operator to Eq. (4) giving

$$\nabla\rho_e = -2\rho_{\max}\left[\left(\frac{x}{x_0^2}\right)\hat{i} + \left(\frac{y}{y_0^2}\right)\hat{j} + \left(\frac{z}{z_0^2}\right)\hat{k}\right]. \quad (8)$$

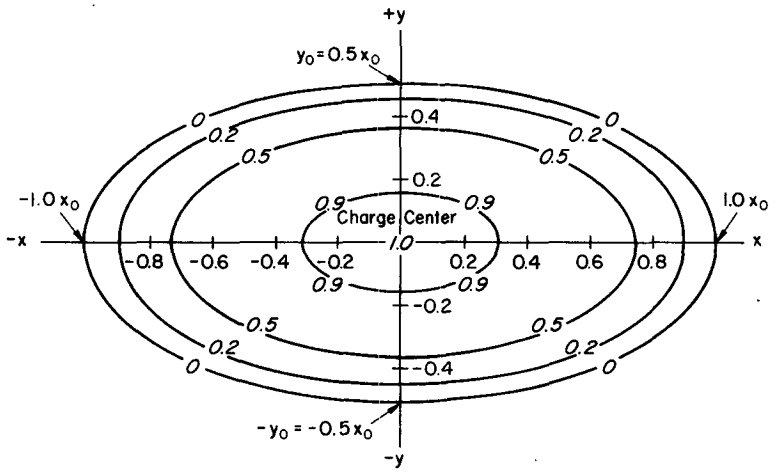

FIG. 1. Ellipsoidal charge distribution at $z = 0$ relative to maximum charge density, ρ_{max} at the center. Semi-major axes, $x_0 = 1.0$, $y_0 = z_0 = 0.5$

Forming the cross product of $\nabla\rho_e$ and E and taking its vertical component, the rate of production of the vertical component of the vorticity is

$$\frac{\partial \eta_{e\uparrow}}{\partial t} = \frac{(\nabla\rho_e \times \mathbf{E})}{\rho_a} \cdot \hat{k}$$

$$= \left[\frac{x_0^2 - y_0^2}{x_0^2 y_0^2}\, xy\left(\frac{1}{3} - \frac{R^2}{5}\right)\right]\left[\frac{2\rho_{max}{}^2}{\rho_a \epsilon_0}\right]. \quad (9)$$

The expression within the first set of brackets in Eq. (9) is plotted in Fig. 2 for the ellipsoidal relative charge density field shown in Fig. 1. With no charge outside the ellipsoid no vorticity is generated there.

The ellipsoidal charge distribution can be modified to allow us to examine two spherical charge distributions ($x_0 = y_0 = z_0 = 1$), for the vorticity created within each of the spheres by the electrical field of the other. Because the field and the charge gradient within the same spherical charged regions are both radial vectors, no vorticity is created within either sphere due to its own charges. For ease of the calculation of the vertical components of vorticity, one of the spheres is centered at the origin of the x, y, z rectangular coordinate system and the other at $x = 2$, $y = 0$, and $z = 0$. This configuration simulates two charged regions aligned side-by-side as might occur in a squall line or a group of air mass thunderstorms. A vertical alignment of the two charged spheres will make no contribution to the vertical vorticity. The charge density in the first sphere is

$$\rho_1 = \rho_{max}[1 - R_1{}^2], \quad (10a)$$

where $R_1{}^2 = x^2 + y^2 + z^2$ and the total charge in this sphere is

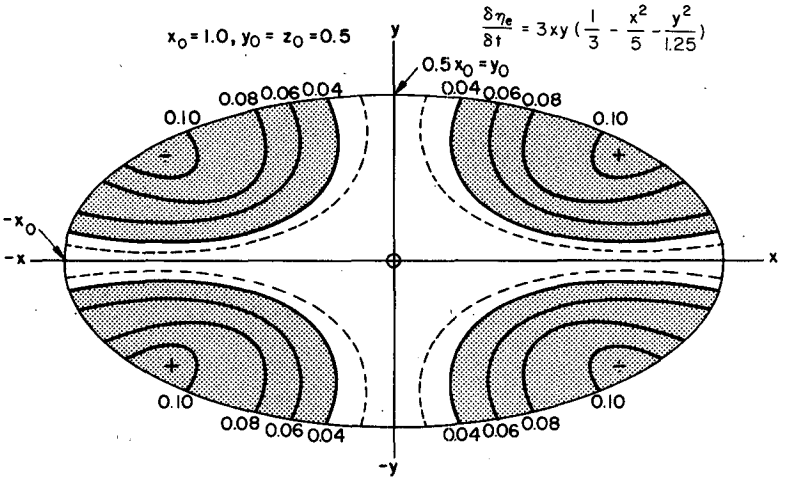

FIG. 2. Rate of change of vertical vorticity (s^{-2}) for charge distribution in Fig. 1 at $z = 0$.

$$q_1 = \rho_{\max} \int_{v_1} (1 - R_1^2) dv_1$$

$$= 4\pi\rho_{\max}\left[\frac{(R_1)_0^3}{3} - \frac{(R_1)_0^5}{5}\right].$$

The charge density in the second sphere is

$$\rho_2 = \rho_{\max}[1 - R_2^2] \tag{10b}$$

which when integrated over the second sphere gives

$$q_2 = 4\pi\rho_{\max}\left[\frac{(R_2)_0^3}{3} - \frac{(R_2)_0^5}{5}\right],$$

where $R_2^2 = (x - 2)^2 + y^2 + z^2$, and $(R_1)_0$ and $(R_2)_0$ are the radii of the two spheres. $\rho_e = 0$, everywhere outside the spheres. If P is an arbitrary point, the electric field on the spheres is given by,

$$\mathbf{E}_1(P) = \frac{q_1}{4\pi\epsilon_0 r_1^2}\hat{U}_{R_1} \quad \text{and} \quad \mathbf{E}_2(P) = \frac{q_2}{4\pi\epsilon_0 R_2^2}\hat{U}_{R_2},$$

where $\hat{U}_{R_1}$ and $\hat{U}_{R_2}$ are unit vectors along a line between the center of each sphere and point P. The field outside each sphere is then given by

$$\mathbf{E}_1 = \frac{\rho_{\max}}{\epsilon_0}\frac{(R_1)_0^3}{R_1^3}\left[\frac{1}{3} - \frac{(R_1)_0^2}{5}\right]\mathbf{R}_1$$

and

$$\mathbf{E}_2 = \frac{\rho_{\max}}{\epsilon_0}\frac{(R_2)_0^3}{R_2^3}\left[\frac{1}{3} - \frac{(R_2)_0^2}{5}\right]\mathbf{R}_2$$

where $\hat{U}_{R_1}$ has been replaced by $\mathbf{R}_1/|\mathbf{R}_1|$ and similarly for $\hat{U}_{R_2}$. The gradient of the charge density is obtained by applying the gradient operator to Eqs. (10a) and (10b)

$$\nabla\rho_1 = -2\rho_{\max}\mathbf{R}_1$$

and

$$\nabla\rho_2 = -2\rho_{\max}\mathbf{R}_2.$$

These equations are the same as those obtained by letting $x_0 = y_0 = z_0 = 1$ in Eqs. (7) and (8) in the case of spheres 1 and 2 and replacing x by $(x - 2)$ in the case of the second sphere. The vertical component of the growth of vorticity of the combined fields is

$$\frac{(\nabla\rho_e \times \mathbf{E})}{\rho_a}\cdot\hat{k} = \frac{1}{\rho_a}[(\nabla\rho_1 + \nabla\rho_2) \times (\mathbf{E}_1 + \mathbf{E}_2)]\cdot\hat{k}$$

$$= \frac{1}{\rho_a}[\nabla\rho_1 \times \mathbf{E}_1 + \nabla\rho_2 \times \mathbf{E}_2 + \nabla\rho_1 \times \mathbf{E}_2 + \nabla\rho_2 \times \mathbf{E}_1]\cdot\hat{k},$$

where $\nabla\rho_1 \times \mathbf{E}_1 = \nabla\rho_2 \times \mathbf{E}_2 = 0$ over spherical distributions, leaving

$$\frac{(\nabla\rho_e \times \mathbf{E})}{\rho_a}\cdot\hat{k} = \frac{1}{\rho_a}[\nabla\rho_1 \times \mathbf{E}_2 + \nabla\rho_2 \times \mathbf{E}_1]\cdot\hat{k}. \tag{11a}$$

However, $\nabla\rho_1 = 0$ everywhere outside $(R_1)_0$ and $\nabla\rho_2 = 0$ everywhere outside $(R_2)_0$, therefore

$$\frac{\partial\eta_{e\uparrow}}{\partial t} = \begin{cases} \dfrac{\nabla\rho_1 \times \mathbf{E}_2}{\rho_a}\cdot\hat{k} & \text{in the region bounded by sphere 1} \\ \dfrac{\nabla\rho_2 \times \mathbf{E}_1}{\rho_a}\cdot\hat{k} & \text{in the region bounded by sphere 2} \\ 0 & \text{elsewhere.} \end{cases} \tag{11b}$$

When the charge gradients and electric fields are entered in equation (11b), setting $(R_1)_0 = (R_2)_0 = 1$ for unit spheres, and the cross product is taken, the expressions for the vertical vorticity production (destruction) in spheres 1 and 2 are given by

$$\left.\begin{aligned} \left(\frac{\partial\eta_{e\uparrow}}{\partial t}\right)_1 &= \frac{8\rho_{\max}^2}{15\epsilon_0\rho_a}\left\{\frac{-y}{[(x - 2)^2 + y^2]^{3/2}}\right\} \\ \left(\frac{\partial\eta_{e\uparrow}}{\partial t}\right)_2 &= \frac{8\rho_{\max}^2}{15\epsilon_0\rho_a}\left\{\frac{y}{(x^2 + y^2)^{3/2}}\right\} \end{aligned}\right\} \tag{12}$$

in the plane $z = 0$. Fig. 3 shows a plot of the bracketed terms for the two spheres.

3. Quantitative results

The average maximum charge density, $\rho_{\max} = \sum_{D=1}^{n} Q_D N_D$, is calculated from observations in thunderstorms. The charge per particle data Q_D of Table 1 are taken from Takahashi's (1973, 1978) observations for moderately charged clouds. These estimates of Q_D are usually one order of magnitude less than the average maximum charge observed by Gunn (1950). Particle concentrations N_D are taken from results of British Meteorological Office research flights (Jones, 1960). The average maximum charges (Takahashi's data increased by 1 order of magnitude) and concentrations are used to calculate the maximum production of the vertical component of vorticity in electrified clouds from Eqs. (9) and (12). The results are presented in Table 2. Table 2 also displays the order of magnitude of vorticity production (on various scales) due to hydrodynamical forces. From this table it may be concluded that except for synoptic scale motion in midlatitudes, the vorticity production due to electrostatic forces in highly charged clouds is comparable to that which is dynamically produced.

The maximum charge densities may be estimated independently from the dipole moment destroyed by a lightning flash in a convective scale thunderstorm. The magnitudes of charge centers in thunderstorms obtained in this way from observations are between 10 and 100 C in two main charge centers of radii about one kilometer each, usually with positive charge above the negative and tilted horizontally with respect to each other by the vertical wind shear in the cloud. The charge density

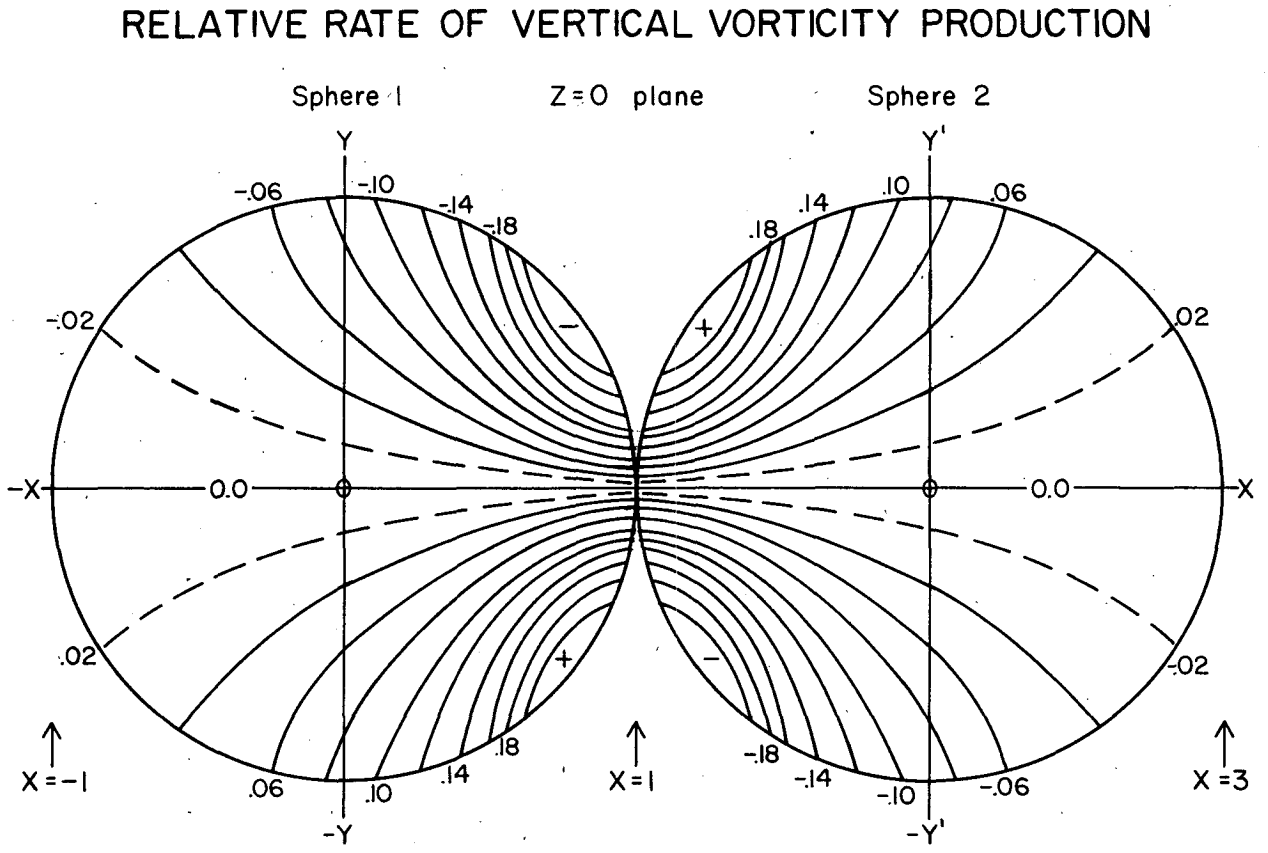

FIG. 3. Rate of change of vertical vorticity (s^{-2}) of a bi-spherical charge distribution at $z = 0$. Sphere centers at $x = y = z = 0$ and $x = 2, y = 0, z = .0$.

maximum is calculated from these data, assuming that the charge centers are spherical and almost touching each other, so that the field outside one center is imposed on the charge distribution of the other. The field created externally by one of these centers where Q is its total charge, R_0 is its radius and R is the radial distance from its center is:

$$E = \frac{Q}{4\pi\epsilon_0 R^2} = \frac{10\text{ C}}{4\pi(8.85 \times 10^{-12})(10^3)^2}$$
$$= 9 \times 10^4\text{ V m}^{-1}$$

to a maximum (100 C) of 9×10^5 V m^{-1}. The maximum average charge density for a spherical distribution is

$$\frac{100\text{ C}}{4/3\pi \times (10^3)^3} = 2.4 \times 10^{-8}\text{ C m}^{-3}.$$

Entering this value in the factor $2(QN)^2/\rho_a\epsilon_0$ of Table 1, and taking $\rho_a = 1$ kg m^{-3},

$$\frac{2\rho_{\max}^2}{\rho_a\epsilon_0} = \frac{2 \times (2.4 \times 10^{-8})^2}{8.85 \times 10^{-12}} = 1.3 \times 10^{-4}\text{ s}^{-2},$$

one order of magnitude larger than the value for the convective scale in Table 1. If the magnitude of the charge center is taken as 10 C, $(2/\rho_a\epsilon_0)\rho_{\max}^2$ is one order of magnitude smaller (1.3×10^{-6}) than the total of this factor for the convective scale (first column) of Table 1. This is an approximate comparison, but is made for an independent source of data and provides a useful check for the calculation summarized in Table 1.

The relative fields of vorticity production for the ellipsoidal charge distribution are shown in Fig. 2 and for the bi-spherical charge distribution in Fig. 3. By multiplying the values in Fig. 2 by $2(\sum QN)^2/\rho_a\epsilon_0$, from Table 1, one obtains the value of the vorticity production at any location within the central plane ($z = 0$) for moderately charged clouds, where the unit distance is the scale length for each cloud or cloud system. A similar set of tabular data can be constructed for the bi-spherical charge distribution by multiplying the $(QN)^2$ values in Table 1 by $^8/_{15}\,\epsilon_0\rho_a$. The relative values in Table 2 are calculated for 0.04 in the case of the ellipsoidal charge distribution while 0.02 is used in the bi-spherical distribution, both covering about ½ the total area of the charged cloud. Again, the maximum values are com-

TABLE 1. Particle size, charge and concentration by meteorological scale and by the maximum average charge density, given by $2\rho_{max}^2/\rho_a\epsilon_0 = 2(QN)^2/\rho_a\epsilon_0$, with $\rho_a = 1$ kg m^{-3} and charge data taken from Takahashi (1973, 1978).

	Convective scale <10 km	Anvil scale 10–100 km	Mesoscale 100–500 km		Synoptic scale 500–5000 km	
			Mid-lat.	Tropics	Mid-lat.	Tropics
$D_{part} = 1.5$ mm						
$Q(C)$	3.33×10^{-12}	3.33×10^{-13}	3.33×10^{-13}	3.33×10^{-13}	3.33×10^{-13}	3.33×10^{-13}
N (m^{-3})	560	560	20	10	1	0.5
$2(QN)^2/\rho_a\epsilon_0$	7.9×10^{-7}	7.9×10^{-9}	1.0×10^{-11}	2.5×10^{-12}	2.5×10^{-14}	6.3×10^{-15}
$D_{part} = 1$ mm						
Q	3.33×10^{-13}	3.33×10^{-13}	3.33×10^{-13}	3.33×10^{-13}	3.33×10^{-13}	3.33×10^{-13}
N	1000	1000	10	50	5	5
$2(QN)^2/\rho_a\epsilon_0$	2.5×10^{-8}	2.5×10^{-8}	2.5×10^{-12}	6.3×10^{-11}	6.3×10^{-13}	6.3×10^{-13}
$D_{part} = 0.5$ mm						
Q	1.67×10^{-13}	1.67×10^{-13}	1.67×10^{-13}	1.67×10^{-13}	3.33×10^{-14}	3.33×10^{-14}
N	5000	1000	100	500	10	50
$2(QN)^2/\rho_a\epsilon_0$	1.6×10^{-7}	6.3×10^{-9}	6.3×10^{-11}	1.6×10^{-9}	2.5×10^{-14}	6.3×10^{-13}
$D_{part} = 0.1$ mm						
Q	1.67×10^{-14}	1.67×10^{-14}	3.33×10^{-15}	3.33×10^{-15}	3.33×10^{-15}	3.33×10^{-15}
N	10^5	10^4	1000	5000	100	500
$2(QN)^2/\rho_a\epsilon_0$	6.3×10^{-7}	6.3×10^{-9}	2.5×10^{-12}	6.3×10^{-11}	2.5×10^{-14}	6.3×10^{-13}
$D_{part} = 10$ μm						
Q	6.67×10^{-17}	6.67×10^{-17}	6.67×10^{-17}	6.67×10^{-17}	6.67×10^{-18}	6.67×10^{-18}
N	5×10^7	5×10^6	10^6	5×10^6	2×10^5	5×10^5
$2(QN)^2/\rho_a\epsilon_0$	2.5×10^{-6}	2.5×10^{-8}	1×10^{-9}	2.5×10^{-8}	4×10^{-13}	2.5×10^{-12}
$2(\Sigma QN)^2/\rho_a\epsilon_0$	1.5×10^{-5}	3.2×10^{-7}	2.1×10^{-9}	4.6×10^{-8}	3.6×10^{-12}	1.6×10^{-11}

puted by increasing the charge values in Table 1 by an order of magnitude and a value of air density $\rho_a = 0.66$ (corresponding to an altitude of 6 km) is used.

The rates of vertical vorticity production calculated from Table 2 for moderately charged particle data (Takahashi, 1978) are of comparable magnitudes only on the cumulonimbus anvil scale and on the

TABLE 2. Comparison of production/destruction of vorticity due to electrical forces and dynamical forces on various scales, for maximum and moderate charges.

		Convective scale 1–10 km Thunderstorm core	Anvil scale 10–100 km Outside thunderstorm core	Mesoscale 100–1000 km		Synoptic scale ≥1000 km	
				Mid-latitude	Tropics	Mid-latitude	Tropics outside Cb
Dynamic		*1	*1	*2	*2		*2
$\frac{\partial\eta}{\partial t_D} \approx U\frac{\Delta\eta}{\Delta L}$		5×10^{-6} to 10^{-5} s^{-2}	10^{-8} to 10^{-7} s^{-2}	10^{-9} s^{-2}	10^{-10} s^{-2}	10^{-10} s^{-2}	3×10^{-12} to 10^{-11} s^{-2}
Electrical	*Maximum*						
Calculated for 6 km*3	Ellipsoidal	8.8×10^{-5}	1.9×10^{-6}	1.3×10^{-8}	2.8×10^{-7}	2.2×10^{-11}	9.9×10^{-11}
$\frac{\partial\eta_1}{\partial t_E}$*4	Bi-Spherical	1.2×10^{-5} s^{-2}	2.6×10^{-7} s^{-2}	1.7×10^{-9} s^{-2}	3.8×10^{-8} s^{-2}	2.9×10^{-12} s^{-2}	1.3×10^{-11} s^{-2}
	Moderate	Multiply above tabular values by 10^{-2}					

*1 Klemp and Wilhelmson (1978a,b).
*2 Holton (1972).
*3 To obtain variation with height multiply tabular values by:

0 km: 0.538 3 km: 0.742 6 km: 1.0 9 km: 1.41 15 km: 3.42 20 km: 7.47

*4 Calculated from Eqs. (9) and (12) with coordinate coefficients of 0.04 and 0.02, respectively. Maximum values obtained by increasing Takahashi (1978) data by one order of magnitude.

mesoscale in the tropics. The results for highly charged particles show that the electrophysical production of vorticity is equivalent to that produced dynamically on all scales except the synoptic scale at midlatitudes. Extensive anvil and mesoscale clouds frequently were observed by the first author during the Winter 1978 and Summer 1979 Monsoon Experiment (MONEX) flights over the South China Sea and the Arabian Sea. The National Center for Atmospheric Research (NCAR) Electra and the National Oceanographic and Atmospheric Administration (NOAA) P-3 aircraft were both struck by lightning in these extensive anvil and mesoscale high clouds. To give some idea of the extent of these clouds, the aircraft flew a number of times at ~140 m s^{-1} for periods of one or more hours on a straight level course at altitudes between 6 and 7 km without leaving cloud at any time.

4. Concluding remarks

Atmospheric forecasters and researchers living in midlatitudes are invariably struck when visiting the tropics by the organization and strong visual evidence of vortical air motions in the cloud systems of the convective and mesoscale circulations there. In the midlatitudes, the Coriolis parameter ($2\Omega \sin\phi$, where Ω is the earth's rotation in radians per second and ϕ is the latitude) is a strong organizing factor on the synoptic and global scales, but it is small in most of the tropics. The departure from geostrophy leaves the dynamic production of vorticity an order of magnitude smaller than in midlatitudes. This could permit organized smaller scale circulations to form and grow electrophysically and to transfer energy from the smaller scales into the larger scales more easily. It could also assist the organization of convective clouds into tropical storms. Some of these disturbances may grow dynamically to hurricane or typhoon strength while linked at critical growth periods to the electrophysical circulation factors in the extensive highly charged cumulonimbus anvil and mesoscale clouds observed over the tropical sense.

It is conceivable that thunderstorms in the midlatitudes and in the tropics contain sufficiently strong horizontal charge density gradients between precipitation shafts and oppositely charged cloud material to lead to vertical vorticity production sufficient to assist or retard the formation of waterspouts and tornadoes. Since the ultimate speed of the circulation is determined by the length of time the vorticity production is applied to the dynamically produced air motions, the effect will be difficult to analyze.

Calculations made in this paper permit the conclusion that the vorticity production in highly charged clouds could be a significant factor in comparison with its dynamic production on the same or larger scales.

Obtaining more definitive calculations of the electrophysical production of vorticity will require more extensive measurements of the particle type, size, and charge and the electric field in clouds under well observed meteorological conditions. Surveys of the physical climatology of cloud types, amounts, and locations would be beneficial in determining where and how suitable the meteorological features are for the application of these electrical processes to the atmosphere.

Further efforts in these directions seem justified in the light of the calculations made in this report.

Acknowledgments. John Helsdon's support to make the required revisions was provided by the Atmospheric Sciences Section, National Science Foundation, under NSF Grant ATM 79-16147.

REFERENCES

Appleton, E. V., and R. Naismith, 1933: Weekly measurements of upper atmospheric ionization. *Proc. Phys. Soc. London*, **45**, 389–399.

Chiu, C.-S., 1978: Numerical study of cloud electrification in an axisymmetric, time-dependent cloud model. *J. Geophys. Res.*, **83**, 5025–5049.

Cobb, W. E., 1967: Evidence of solar influence on the atmospheric electric elements at Mauna Loa Observatory. *Mon. Wea. Rev.*, **95**, 905–911.

Gunn, R., 1950: The free electrical charge on precipitation inside an active thunderstorm. *J. Geophys. Res.*, **55**, 171–178.

Hays, P. B., and R. B. Roble, 1979: A quasi-static model of global atmospheric electricity. 1. The lower atmosphere. *J. Geophys. Res.*, **84**, 3291–3305.

Herman, J. R., and R. A. Goldberg, 1978: Initiation of non-tropical thunderstorms by solar activity. *J. Atmos. Terr. Phys.*, **40**, 121–134.

Holton, J. R., 1972: *An Introduction to Dynamic Meteorology*. Academic Press, 319 pp.

Isted, A., 1954: Atmospheric electricity and long distance very high frequency scalar transmissions. *Marconi Rev.*, **7**, 37–60.

Jones, R. F., 1960: Size-distribution of ice crystals in cumulonimbus clouds. *Quart. J. Roy. Meteor. Soc.*, **86**, 187–194.

Klemp, J. B., and R. B. Wilhelmson, 1978a: The simulation of three-dimensional convective storm dynamics. *J. Atmos. Sci.*, **35**, 1070–1096.

——, and ——, 1978b: Simulations of right- and left-moving storms produced through storm splitting. *J. Atmos. Sci.*, **35**, 1097–1110.

Kuettner, J., Z. Levin and D. Sartor, 1978: Inductive or noninductive electrification of thunderstorms. *Preprints Conf. on Cloud and Atmospheric Electricity*, Issaquah, Amer. Meteor. Soc., 649–654.

Markson, R., 1978: Solar modulation of atmospheric electrification and possible implications for the sun–weather relationship. *Nature*, **273**, 103–109.

Mason, B. J., 1972: The physics of thunderstorms. *Proc. Roy. Soc. London*, **A327**, 433–466.

National Science Foundation, 1978: The sun the whole sun. MOSAIC, Jan./Feb., 8–16.

Paluch, I. R., and J. D. Sartor, 1973: Thunderstorm electrifica-

tion by the inductive charging mechanism: I. Particle charges and electric fields. *J. Atmos. Sci.*, **30,** 1166–1173.

Reiter, R., 1969: Solar flares and their impact on potential gradient and air-earth current characteristics at high mountain stations. *Pure Appl. Geophys.*, **72,** 259–267.

——, 1971: Further evidence for impact of solar flares on potential gradient and air-earth current characteristics at high mountain stations. *Pure Appl. Geophys.*, **86,** 142–158.

——, 1976: The electrical potential of the ionosphere as controlled by the solar magnetic sector structure. *Naturwissenschaften,* **63,** 192.

Roberts, W. O., and R. H. Olson, 1973: Geomagnetic storms and wintertime 300-mb trough development in the North Pacific–North America area. *J. Atmos. Sci.*, **30,** 135–140.

Sartor, J. D., 1967a: The role of particle interactions in the distribution of electricity in thunderstorms. *J. Atmos. Sci.*, **24,** 601–615.

——, 1967b: The remote sensing of radio emission from convective clouds, including transmission via sporadic E. *Mon. Wea. Rev.*, **95,** 871–877.

——, 1970: Accretion rates of cloud drops, raindrops, and small hail in mature thunderstorms. *J. Geophys. Res.*, **75,** 7547–7558.

——, 1980: Electric field perturbations in terrestrial clouds and solar flare events. *Mon. Wea. Rev.*, **108,** 499–505.

Scott, W. D., and Z. Levin, 1975: A stochastic electrical model of an infinite cloud: charge generation and precipitation. *J. Atmos. Sci.*, **32,** 1814–1828.

Takahashi, T., 1973: Measurements of electric charge of cloud droplets, drizzle, and raindrops. *Rev. Geophys. Space Phys.*, **11,** 903–924.

——, 1978: Electrical properties of oceanic tropical clouds at Ponape, Micronesia. *Mon. Wea. Rev.*, **106,** 1598–1612.